

# 2

## ***Hydrogen Storage using Physisorption - Materials Demands***

### **Abstract**

A survey is presented of the hydrogen storage capacities of a large number of different adsorbents at 77 K and 1 bar. Results are evaluated to examine the scope of storage based on physisorption of hydrogen on solid adsorbents. It is concluded that microporous adsorbents, e.g. zeolites and activated carbons, display appreciable sorption capacities. Based on their micropore volume (~1 ml/g) carbon-based sorbents display the largest adsorption capacity, viz. 238 ml (STP)/g, at the prevailing conditions. Optimisation of sorbent and adsorption conditions is expected to lead to adsorption of ~560 ml (STP)/g, close to targets set for mobile applications.

## 2.1 Introduction

In the last two decades there has been an increasing interest in the development of (transportable) reversible systems for hydrogen storage with a high capacity, which is critical to the large-scale application of hydrogen fuel cells in particular for mobile applications [1]. Up to now focus has mostly been on liquid hydrogen, pressurized hydrogen and metal hydrides systems, which all have low energy efficiencies [2]. The energy efficiency of these systems is at most 80%. A higher energy efficiency (90%) is attainable with systems in which hydrogen is concentrated by physical adsorption above 70 K using a suitable adsorbent [3-5]. Such an adsorbent should be safe, light and cheap and of course have a high adsorption capacity. In order to obtain a suitable driving range for automotive applications the United States Department of Energy (DOE) target has been set to 6.5 wt% H<sub>2</sub>, which equals 720 ml (STP) H<sub>2</sub>/g<sub>ads</sub>. Schwarz and co-workers [6-8] studied the applicability of molecularly engineered activated carbons and came with promising results. Much excitement has arisen from recent reports on the use of carbon nanofibers [9,10] and carbon nanotubes [11,12] but because of further research [13] the exciting results have become questionable. Chapter 1 deals with these reports in more detail.

In this chapter we present a survey of the storage capacity for molecular hydrogen at 77 K and 1 bar of a large number of different types of adsorbents, such as silicas, aluminas, zeolites, graphite, activated carbons and carbon nanofibers. Care has been taken to make sure that these adsorbents include a wide range of specific surface areas and different textures. The carbon nanofibers, aerosil and graphite are materials, which structure only contains large mesopores and macropores. We have studied an all silica material, MCM-41, which completely consists of very regular, 3 nm diameter pores. Some of the activated carbons are mesoporous as well. The zeolites, activated graphite, activated carbon fibers and activated carbon that were studied, are microporous materials. It was made sure that this selection contained materials with small micropores, ~1 nm diameter, as well as materials with larger (super-) micropores, between 1 and 2 nm diameter. The materials were not modified to change their adsorptive properties before their hydrogen adsorption capacity was measured.

## 2.2 Experimental

A large number of carbonaceous (see table 2.1) and silica-alumina based (see table 2.2) sorbents were characterized using N<sub>2</sub> physisorption at 77 K and up to a pressure of 1 bar. The sorbents were chosen to represent a large variation in surface areas and (micropore) volumes. The materials were used as synthesized, or as obtained commercially, without modification to change their adsorptive properties. Both non-microporous materials, such as aerosil and graphites, and microporous sorbents, such as activated carbons and zeolites, were selected. First we provide a brief description of the samples selected with the sample numbers between brackets. Activated carbons are highly micro- and mesoporous carbon materials. They have been steamed or chemically activated. Steam-activated carbons (7,8,11,12,14-19) have been

prepared from raw materials (e.g. peat, lignite, coal) and carbonized and reacted with steam at 1000°C. In this way part of the carbon atoms are removed by gasification, which yields a very porous structure. Chemically activated carbons (20) are produced by mixing an activation chemical (usually phosphoric acid) with a young carbonaceous material (usually sawdust), and carbonizing the resultant mixture at 500°C. The resulting very porous carbon structure is filled with activation agent, which is removed from carbon by washing [14]. Activated carbon fibers (5,6,12) have been prepared by controlled pyrolysis of various structures, e.g. the synthetic polymer polyacrylonitrile (PAN) or coal-tar pitch [15]. These fibers are subsequently subjected to activation as described for the activated carbons. Activated graphite (3,9) is synthetic graphite which has been activated in the same way as described for the activated carbons. Carbon nanofibers (2,4,10,21) have been catalytically synthesized, as described in chapter 3. These fibers consist of conical (fishbone, 2,4,10) or tubular (parallel, 21) graphite planes [16]. Zeolites are highly crystalline, microporous materials, consisting of silica and alumina. Zeolite L (23) consists of uni-dimensional 12-ring pores, with 0.9 nm diameter. Ferrierite (25) is a two dimensional pore network, consisting of pseudo-spherical cages with 8-ring openings (0.35\*0.48 nm) and interconnecting 10-ring pores (0.42\*0.55 nm). ZSM-5 (24) consists of tri-dimensional interconnecting 10-ring pores of dimensions 0.51\*0.55 nm [17]. The silicas and aluminas (22,26-34,36) are all commercially available inert catalyst supports selected for their lack of microporosity. MCM-41 (35) is an all-silica material, consisting of highly regular, 3 nm diameter channels [18,19].

From the N<sub>2</sub> physisorption data, obtained with a Micromeritics ASAP 2400 apparatus, the BET surface area, total pore volume (PV), micropore volume (MPV) and t-surface (S<sub>t</sub>) were derived. All pore volumes are expressed in ml/g, the micropore volume is defined as the pore volume of the pores < 2 nm. The BET surface area (S<sub>BET</sub>, m<sup>2</sup>/g) is the surface area of the sorbent according to the model formulated by Brunauer, Emmet and Teller [13] for planar surfaces. The BET-equation is formulated to assess multilayer adsorption of small inert molecules on substrates. The t-surface area (S<sub>t</sub>, m<sup>2</sup>/g) is derived from the t-plot and is the mesoporous (> 2 nm) surface area of the sorbent, i.e. the surface area excluding the micropores [20].

The H<sub>2</sub> adsorption measurements were performed volumetrically with a Micromeritics ASAP 2010 at 77 K in the pressure range 0-1 bar. From adsorption-desorption experiments it is evident that reversible physisorption exclusively takes place with all samples.

The micropore analysis was also performed with a Micromeritics ASAP 2010 at 77 K in the pressure range 0-1 bar with nitrogen. The pore diameters, assuming slit-shaped pores, were calculated with the DFTPLUS algorithm provided by Micromeritics.

## 2.3 Results and discussion

The results of the N<sub>2</sub>- and H<sub>2</sub>-physisorption measurements are shown in table 2.1 and 2.2. In these tables CNF is used to designate carbon nanofibers, ACF is used for activated carbon fibers and AC for activated carbon. Representative adsorption isotherms are shown for oxides (figure 2.1) and carbon materials (figure 2.2).

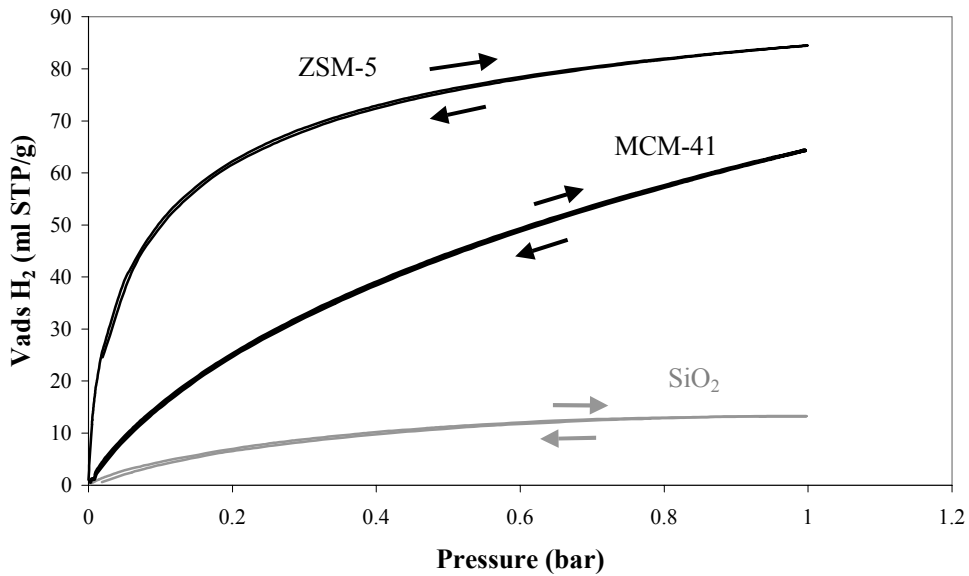


Figure 2.1 Adsorption isotherms for aerosil, MCM-41 and zeolite (ZSM-5).

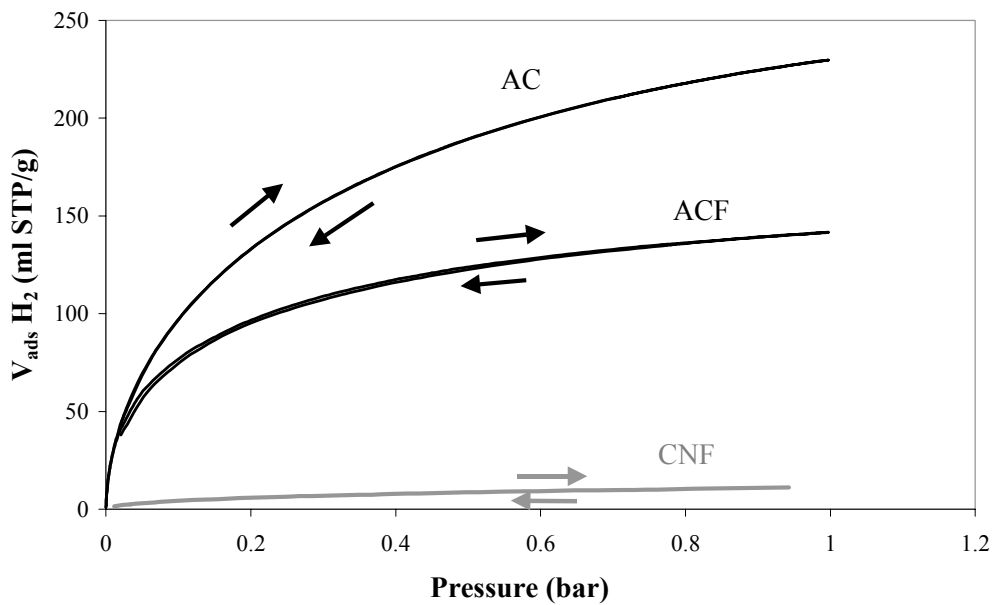


Figure 2.2 Adsorption isotherms for CNF, ACF and AC.

Table 2.1 Texture analysis and hydrogen adsorption capacities at 77 K and 1 bar for carbonaceous materials.

No.	Material	PV (ml/g)	S <sub>BET</sub> (m <sup>2</sup> /g)	S <sub>t</sub> (m <sup>2</sup> /g)	MPV (ml/g)	H <sub>2</sub> total (ml (STP)/g)	H <sub>2</sub> meso (ml (STP)/g)	H <sub>2</sub> micro (ml (STP)/g)
1	Synth. graphite	0.04	7	7	0.00	0	0	0
2	Large diam. CNF	0.10	49	26	0.01	6	2	4
3	Act. Graphite 100	0.26	119	85	0.02	14	6	8
4	Medium diam. CNF1	0.28	120	120	0.00	12	11	1
5	ACF 400	0.40	883	12	0.34	143	1	142
6	ACF 1200	0.42	899	7	0.37	184	1	183
7	AC Norit 990721	0.43	988	17	0.43	142	2	140
8	AC Norit ROZ 3	0.50	287	84	0.05	36	6	28
9	Act. Graphite 300	0.51	287	183	0.05	36	16	19
10	Medium diam. CNF2	0.55	65	65	0.00	7	7	0
11	AC Norit SX 2	0.60	841	194	0.27	150	17	133
12	ACF 500	0.61	988	173	0.40	142	15	127
13	AC Norit UOK A	0.65	1195	110	0.47	188	10	178
14	AC Norit SX 1	0.67	922	206	0.31	168	18	150
15	AC Norit SX 1G AIR	0.68	1030	180	0.36	171	16	155
16	AC Norit GSX	0.78	933	302	0.26	161	27	134
17	AC Norit SX plus	0.79	1051	238	0.35	165	21	144
18	AC Norit SX 1 G	0.83	1176	229	0.40	187	20	167
19	AC Norit 990293	1.03	2029	78	0.92	238	7	231
20	AC Norit Darco KB	1.39	1462	610	0.42	146	54	92
21	Hyperion CNF	2.75	238	238	0.00	22	22	0

Table 2.2 Texture analysis and hydrogen adsorption capacities at 77 K and 1 bar for oxides.

No.	Material	PV (ml/g)	S <sub>BET</sub> (m <sup>2</sup> /g)	S <sub>t</sub> (m <sup>2</sup> /g)	MPV (ml/g)	H <sub>2</sub> total (ml (STP)/g)	H <sub>2</sub> meso (ml (STP)/g)	H <sub>2</sub> micro (ml (STP)/g)
22	SiO <sub>2</sub> 90	0.23	79	64	0.01	4	4	0
23	Zeolite L	0.25	344	26	0.12	59	1	58
24	Zeolite ZSM5	0.28	431	43	0.16	80	2	78
25	Zeolite ferrierite	0.32	344	41	0.12	65	2	63
26	SiO <sub>2</sub> D051A	0.48	172	172	0.00	9	9	0
27	SiO <sub>2</sub> 1614E	0.51	97	97	0.00	9	9	0
28	SiO <sub>2</sub> Caboxil M5	0.59	185	183	0.00	11	11	0
29	S980G	0.60	67	67	0.00	5	5	0
30	SiO <sub>2</sub> Aerosil 200	0.66	167	167	0.00	0	0	0
31	SiO <sub>2</sub> Becker AD 050	0.74	330	330	0.00	18	18	0
32	SiO <sub>2</sub> -60-1	0.75	61	52	0.00	3	3	0
33	Al <sub>2</sub> O <sub>3</sub> preshaped	0.80	233	233	0.00	7	7	0
34	SiO <sub>2</sub> 380	0.87	322	273	0.03	27	15	12
35	MCM-41	1.04	1017	1017	0.00	65	65	0
36	S970SH	1.08	290	268	0.01	28	15	13

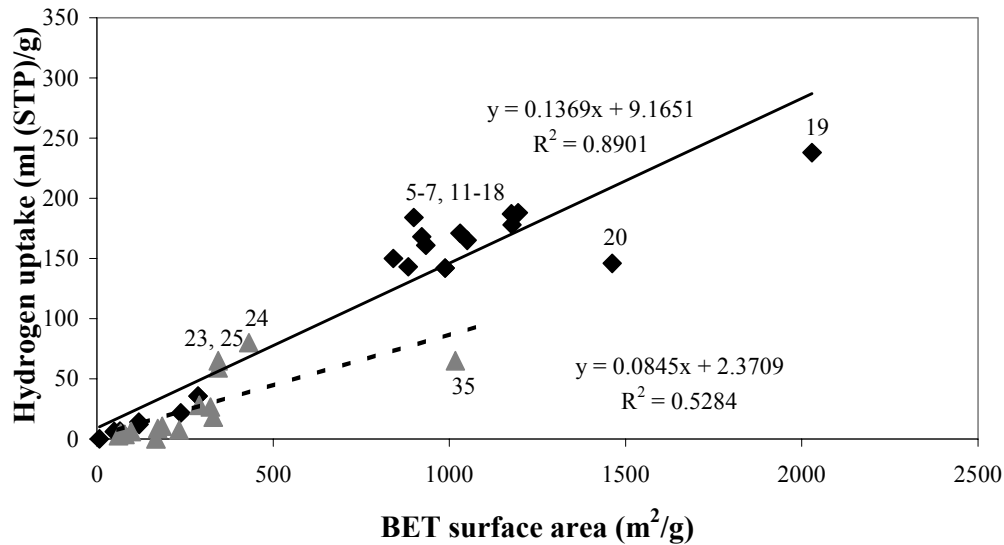


Figure 2.3 Hydrogen adsorption versus at BET surface area 77 K and 1 bar for carbon (◆), silica and alumina (▲).

In a first approach the total amounts of hydrogen taken up per gram of adsorbent at 77 K and 1 bar are correlated with  $S_{\text{BET}}$ . From figure 2.3 it can be concluded that this correlation exist, but is not very straightforward. It is apparent that with the mesoporous silicas and aluminas a low  $\text{H}_2$  capacity is found, even with the MCM-41 sample (35) exhibiting a  $S_{\text{BET}}$  of 1017  $\text{m}^2/\text{g}$ . Only with the zeolites (23,24,25), with  $S_{\text{BET}}$  values of 344, 431 and 344  $\text{m}^2/\text{g}$ , an enhanced capacity, relative to the linear correlation for oxides, is measured, probably because of their microporous texture. This also holds for the mainly microporous carbon samples (5-7,11-18).

Above results suggest that a better correlation is to be expected between the micropore volumes and the respective adsorption capacities for  $\text{H}_2$ . However, it is important to realize that hydrogen not exclusively adsorbs in the micropores but also on the surface of the mesopores. Therefore, to find the actual  $\text{H}_2$ -uptake in the micropores we have corrected the total  $\text{H}_2$  uptakes for the amounts adsorbed on the mesopore surface area.

We calculated the contribution by the mesopores using the correlation which exists, as shown in figure 2.4, between the adsorbed volumes and the t-surfaces of the various non-microporous silica (27,31), alumina (29) and carbon samples (4,10,21, all carbon nanofibers). Obviously hydrogen adsorbs more strongly on carbon surfaces: the oxidic surfaces take up 0.06 ml (STP)/ $\text{m}^2$  at 1 bar, the carbon surfaces 0.09 ml (STP)/ $\text{m}^2$ . Using the above correlations and the t-surface areas as derived from the  $\text{N}_2$  physisorption measurements the surface coverage of  $\text{H}_2$  at 1 bar can be calculated, if the average area, occupied by one  $\text{H}_2$  molecule ( $a_{\text{M}}$ ) is known. Following the approach of Emmet and Brunauer [21], we estimated  $a_{\text{M}}$  to be 0.14  $\text{nm}^2$ . With this a monolayer capacity for  $\text{H}_2$  can be calculated of  $7.10^{18}$  molecules/ $\text{m}^2$ . Thus, for the oxidic surfaces we arrive, at 77 K, at a coverage of 22% while with the carbon surfaces a coverage of 34% is attained at 1 bar.

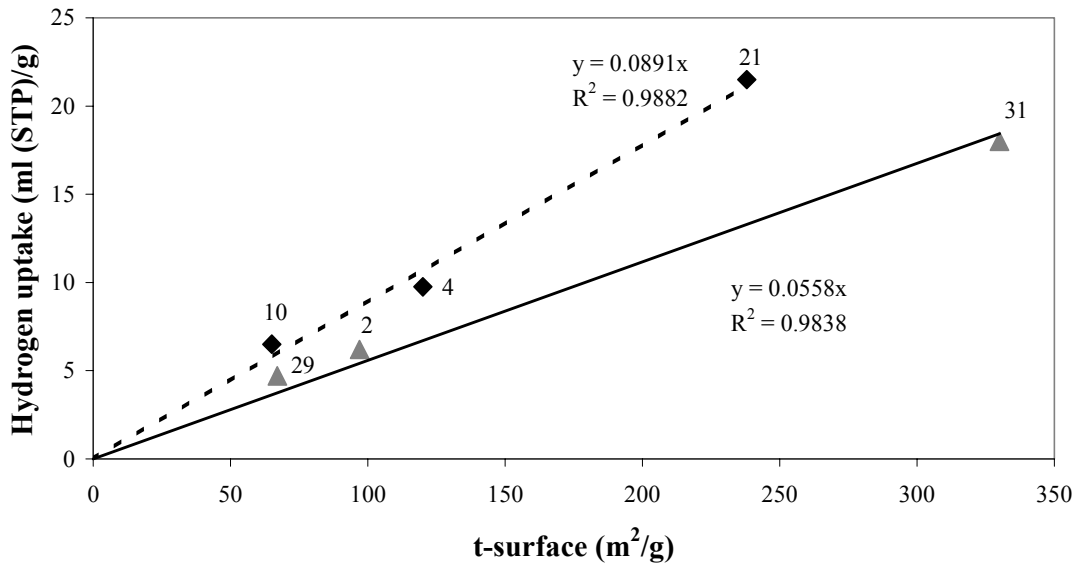


Figure 2.4 Hydrogen adsorption versus t-surface at 77 K and 1 bar for carbon (◆), silica and alumina (▲).

In figure 2.5 the t-surface corrected hydrogen uptakes of various microporous silica (34), alumina (36) and zeolite (23,24,25) samples are plotted against their micropore volumes.

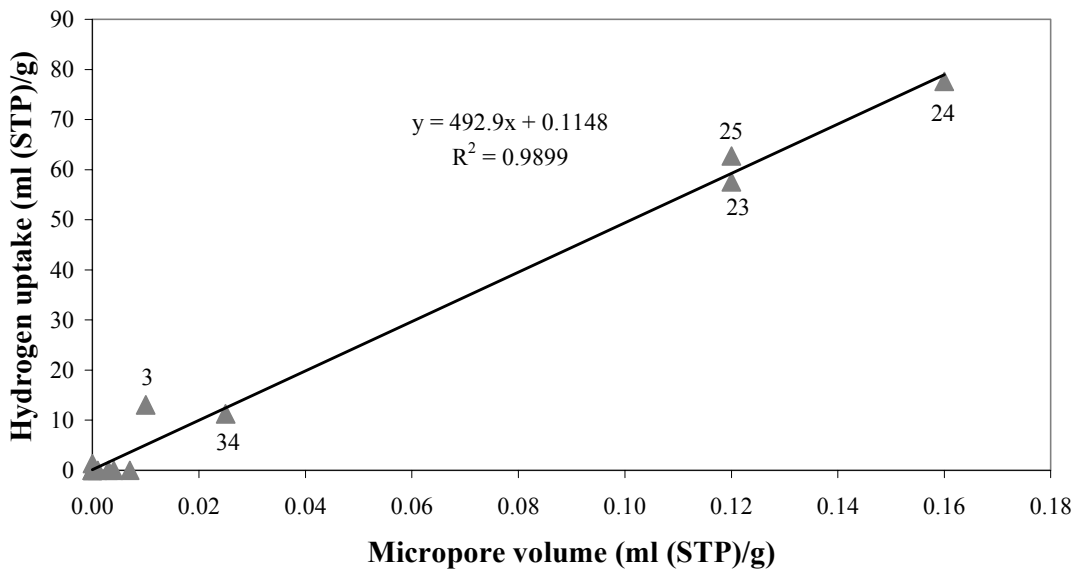


Figure 2.5 t-surface corrected hydrogen adsorption versus micropore volume at 77 K and 1 bar for silica and alumina.

In figure 2.6 this is shown for the microporous carbon samples.

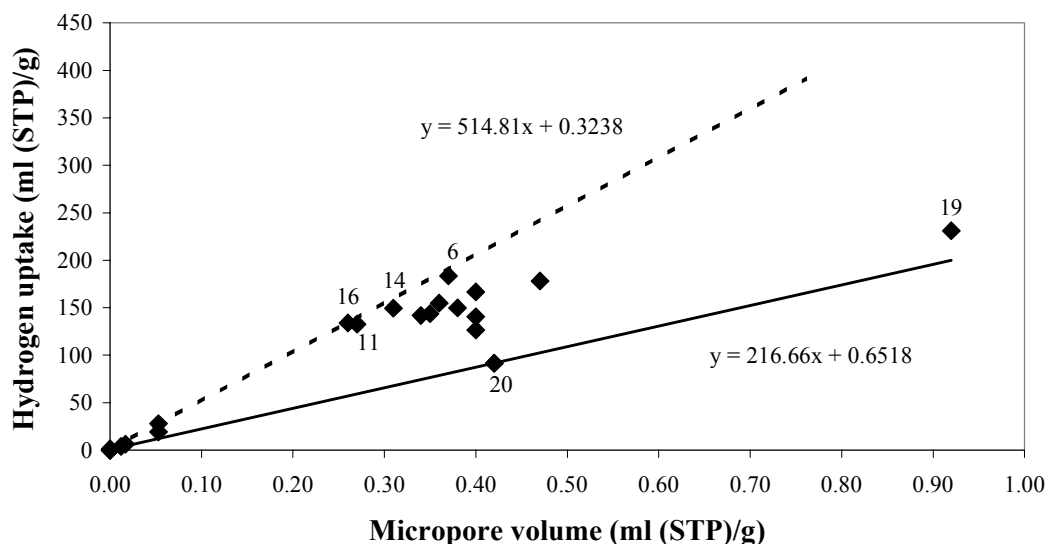


Figure 2.6 *t*-surface corrected hydrogen adsorption versus micropore volume at 77 K and 1 bar for carbon.

A good correlation is found with the oxidic samples (figure 2.5). The scatter of the data points at low hydrogen uptakes is due to the relatively large error in the calculated micropore volumes. Based on the derived linear correlation the H<sub>2</sub> uptake per ml of micropore volume amounts to 490 ml (STP)/g. The apparent density of H<sub>2</sub> inside the zeolite micropores amounts to 0.044 g/ml, that is 63% of the density of liquid hydrogen (0.07 g/ml). For carbon-based sorbents a large scatter between the data for the H<sub>2</sub> uptake and the micropore volume is observed (figure 2.6). A lower limit for the correlation is given mainly by samples 19 and 20. The lower line shown in figure 2.6 relates to an H<sub>2</sub> uptake of 220 ml (STP)/ml or an H<sub>2</sub> density of 0.020 g/ml (28% of liquid H<sub>2</sub>). The upper limit (6,11,14,16) gives 515 ml (STP)/ml or a H<sub>2</sub> density of 0.046 g/ml (66% of liquid H<sub>2</sub>). For microporous carbons the details of the pores (size and shape) apparently affect the specific H<sub>2</sub> uptake to a large extent.

A preliminary study to relate the effect of the details of the microporosity to the specific H<sub>2</sub> uptake is reported. Using DFT calculations and assuming slit-shaped pores the pore diameter distributions have been established. The calculated pore sizes range from 0.5 to 2.0 nm (table 2.3, figure 2.7). Realizing that the results have been obtained from N<sub>2</sub> physisorption (N<sub>2</sub> molecule diameter ~0.4 nm), the ‘resolution’ of the technique is not better than ~0.4 nm. However, the samples 13 and 19 containing super-micropores (1-2 nm) give rise to a lower average H<sub>2</sub> density in the pores than samples 5-12 (0.5-1 nm pores). Tentatively, we conclude that micropores < 1 nm are beneficial to enhance H<sub>2</sub> uptake capacity. At a molecular scale, this implies that graphite structures with 2-3 graphene sheets missing are desirable.

Table 2.3 Pore diameters of several carbon compounds.

No.	Material	Average pore diameter (nm)	H <sub>2</sub> density (g/ml)
5	ACF 400	0.5-0.8	0.038
6	ACF 1200	0.6-0.8	0.046
7	AC Norit 990721	0.8-1.0	0.029
12	ACF 500	0.7-1.0	0.029
13	AC Norit UOK A	0.9-1.5	0.034
19	AC Norit 990293	0.8-2.0	0.023

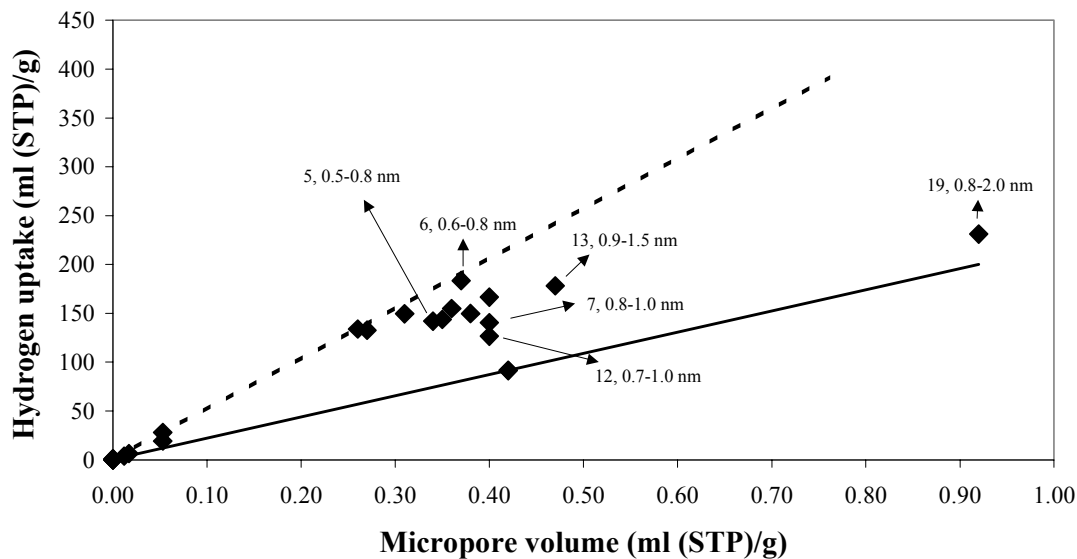


Figure 2.7 Corrected H<sub>2</sub> uptake versus micropore volume of carbon compounds, with diameters of the micropores of several of these carbon compounds reported.

However, the used method for the determination of the pore diameter has limitations and possibly the accuracy of the results could be improved by using another method. Recently a lot of research has been performed on determination of pore sizes with adsorption isotherms, using other computational methods or different adsorption gasses [22-30]. It should be possible to find a more suitable method or adsorption gas to probe the dimensions of these micropores. If so, it would be possible to draw more definitive conclusions on the most suitable pore dimensions for hydrogen storage. Another possibility is that not only the size, but also the specific shape of the pores has a large influence on the adsorption capacity.

In comparing microporous oxides (zeolites) and carbons (activated carbons) it turns out that similar hydrogen densities (0.04-0.05 ml/g) are observed at 77 K and 1 bar. For mesoporous surfaces (figure 2.5) carbon interacts somewhat stronger with H<sub>2</sub> than oxides do. For micropores this difference vanishes, probably due to the different shape of the micropores for activated carbons (slits) and zeolites (cylinders). The main advantage of carbon over oxides resides with the range of micropore volumes that can realistically be achieved. Zeolites with a micropore volume of say 0.5 ml/g or above do not exist, whereas with activated carbon 1 ml/g is common practice. The details of the pore size and shape are very important with the latter, though.

The importance of the size of pores in hydrogen uptake can be illustrated further with the hydrogen adsorption capacity of MCM-41. This oxidic material has very regular, 3 nm diameter pores, which makes it a completely mesoporous material. It adsorbs 65 ml (STP)/g, which is a 12% higher uptake than found with other mesoporous oxides (see table 2.2). This shows that the hydrogen in the mesopores of MCM-41 is slightly more stabilized than by other oxidic mesoporous surfaces. It is however not stabilized as much as H<sub>2</sub> in micropores of zeolites (see figure 2.3).

The density of H<sub>2</sub> in the micropores of carbon at the prevailing conditions (77 K, 1 bar) ranges from 0.02-0.05 g/ml, that is 30-70% of the density of liquid H<sub>2</sub>. With the current types of carbon sorbents at the prevailing sorption conditions a maximum uptake of 238 ml (STP)/g has been measured, amply below the DOE target of 720 ml (STP)/g for mobile applications. In case we could realize a micropore volume of 1 ml/g, with a H<sub>2</sub> density of 0.05 g/ml the uptake would rise to 560 ml (STP)/g, much closer to the DOE target. By optimization of both sorbent and sorption conditions (P, T) the H<sub>2</sub> density might approach that of liquid H<sub>2</sub> giving rise to an uptake of 780 ml (STP)/g.

## 2.4 Conclusions

Our results demonstrate that a large storage capacity for hydrogen by physisorption under the chosen conditions (77 K, 1 bar) is only obtained with adsorbents containing a large volume of micropores with a suitable diameter. Although with zeolite-like materials the chance to find an optimal pore diameter seems realistic, their unavoidably limited micropore volume makes their applicability less likely. With carbonaceous adsorbents (e.g. activated carbons) a more optimistic perspective can be offered. Their intrinsic interaction with hydrogen seems to be slightly stronger than that with oxidic adsorbents, their micropore volume can probably be increased to a value above 1 ml/g, while by increasing the storage pressure or by tuning the pore diameter the storage capacity can be raised up to the targets set for mobile applications. Because of the various sizes and shapes of the micropores in activated carbon it is as yet impossible to comment in details on the optimum pore size and shape. Preliminary results indicate that pores of 0.5-1.0 nm are more beneficial than those of 1.0-2.0 nm. Future research should be focused on a more precise identification of the optimal pore diameter and on the

development of experimental procedures to provide carbon materials with a high volume of these suitable pores.

For our research it is decided that an adsorbent has to be created with a micropore volume as large as possible in order to achieve a high hydrogen storage capacity. We choose a carbon material, because with carbon intrinsically a much higher micropore volume can be attained than with a silica or alumina material. To create micropores the space between subsequent graphene sheets in graphite has to be enlarged. An option to achieve this is via intercalation. A lot of different materials can be intercalated into graphite, for instance alkali metals and metal halides [31,32]. We expect that if we enlarge the d-spacing to 1 nm we may attain enhanced hydrogen storage capacity, based on the results of calculations done by Darkrim *et al.* [33], Rzepka *et al.* [34] and Wang *et al.* [35]. Because we aimed at the development of a material which is suitable as a hydrogen storage device for automotive applications, the material also must be strong. Carbon nanofibers are mechanically strong [16] and may meet the demands for automotive applications. The fibers have the added advantage of short graphite planes, which can diminish diffusion times of the hydrogen into the adsorbent. This will shorten re-fuelling times and problems with hydrogen to fuel cell diffusion inside the car. The results of these intercalation experiments with carbon nanofibers and graphite and the influence on the hydrogen adsorption capacity are described for iron(III)-chloride in chapter 5 and potassium in chapter 6.

## Acknowledgements

We wish to acknowledge John Raaymakers for performing the N<sub>2</sub> and H<sub>2</sub> physisorption measurements. We would like to thank Norit for providing the activated carbons. We would like to thank dr. Ben Dekkers for discussions about the BET results.

## References

1. G.D. Berry and S.M. Aceves, *Energy Fuels* 12 (1998) 49.
2. G. Sandroock, *Journal of Alloys and Compounds* 293-295 (1999) 877.
3. C.C. Ahn, Y. Ye, V. Ratnakumar, C. Witham, R.C. Bowman, Jr. and B. Fultz, *Proceedings of the Battery Conference on Applications and Advances* 14 (1999) 67.
4. C. Nutzenadel, A. Zuttel, D. Chartouni and L. Schlapbach, *Electrochemical and Solid State Letters* 2 (1999) 30.
5. F. Darkrim and D. Levesque, *The Journal of Physical Chemistry B* 104 (2000) 6773.
6. K.A.G. Amankwah and J.A. Schwarz, *International Journal on Hydrogen Energy* 14 (1989) 437.
7. J. Jagiello, T.J. Bandosz, K. Putyera and J.A. Schwarz, *Journal of the American Chemical Society, Faraday Transactions* 91 (1995) 2929.
8. J.A. Schwarz, J.S. Noh and R.K. Argawal, *United States Patent* 4,960,450 (1990).
9. A. Chambers, C. Park, R.T.K. Baker and N.M. Rodriguez, *The Journal of Physical Chemistry B* 102 (1998) 4253.
10. C. Park, P.E. Anderson, A. Chambers, C.D. Tan, Hidalgo and R. Rodriguez, *Journal of Physical Chemistry B*. 103 (1999) 10572.
11. A.C. Dillon, K.M. Jones, T.A. Bekkedahl, C.H. Kiang, D.S. Bethune and M.J. Heben, *Letters to Nature* 386 (1997) 377.
12. M.J. Heben, A.C. Dillon, J.L. Alleman, K.M. Jones and P.A. Parilla, *Abstracts 2000 MRS Fall Meeting*, p. 17.
13. M. Hirscher, M. Becher, M. Haluska, U. Dettlaff-Weglikowska, A. Quintel, G.S. Duesberg, Y.-M. Choi, P. Downes, M. Hulman, S. Roth, I. Stepanek and P. Bernier, *Applied Physics A* 72 (2001) 129.
14. *Heterogeneous Catalysis for the Synthetic Chemist*, R.L. Augustine (Marcel Dekker, Inc., 1996) p. 167.
15. *Carbon nanotubes and related structures*, P.J.F. Harris (Cambridge University Press, 1999) p. 187.
16. K.P. de Jong and J.W. Geus, *Catalysis Reviews- Science and Engineering* 42 (2000) 481.
17. *Catalysis and Zeolites*, J. Weitkamp and L. Puppe (Springer-Verlag Berlin Heidelberg, 1999) p. 288.
18. A.T. Kresge, M.E. Leonowicz, W.J. Roth, J.C. Vartuli and J.S. Beck, *Nature* 359 (1992) 710.
19. J.S. Beck, J.C. Vartuli, W.J. Roth, M.E. Leonowicz, C.T. Kresge, K.D. Schmitt, C.T.-W. Chu, D.H. Olson, E.W. Sheppard, S.B. McMullen, J.B. Higgins and J.L. Schlenker, *Journal of the American Chemical Society* 114 (1999) 10834.
20. A.C. Lippens, B.G. Linsen and J.H. De Boer, *Journal of Catalysis* 3 (1964) 32.
21. P.H. Emmett and S. Brunauer, *Journal of the American Chemical Society* 59 (1937) 1553.
22. F. Stoeckli, A. Guillot, D. Hugi-Cleary and A.M. Slassi, *Carbon* 38 (2000) 929.
23. P.I. Ravikovitch, A. Vishnyakov, R. Russo and A.V. Neimark, *Langmuir* 16 (2000) 2311.
24. T. Ohba, T. Suzuki and K. Kaneko, *Carbon* 38 (2000) 1879.
25. M. El-Merraoui, M. Aoshima and K. Kaneko, *Langmuir* 16 (2000) 4300.
26. R.H. Bradley, I. Sutherland and E. Sheng, *Journal of Colloid and Interface Science* 179 (1996) 561.

27. K. Wang and D.D. Do, *Langmuir* 13 (1997) 6226.
28. J. Jagiello, T.J. Bandosz and J.A. Schwarz, *Langmuir* 12 (1996) 2837.
29. M. Jaroniec and J. Choma, *Colloids and Surfaces* 37 (1989) 183.
30. K. Kaneko, *Journal of Membrane Science* 96 (1994) 59.
31. H. Selig and L.B. Ebert, *Advances in Inorganic Chemistry and Radiochemistry* 23 (1980) 281.
32. P.C. Ecklund, *NATO ASI Series, Series B 148 (Intercalation Layered Materials)* (1986) 309.
33. F. Darkrim and D. Levesque, *Journal of Chemical Physics* 109 (1998) 4981.
34. M. Rzepka, P. Lamp and M.A. de la Casa-lillo, *Journal of Physical Chemistry B* 102 (1998) 10894.
35. Q. Wang and J.K. Johnson, *The Journal of Physical Chemistry B* 103 (1999) 277.